

Novel *N*-Substituted Oseltamivir Derivatives as Potent Influenza Neuraminidase Inhibitors: Design, Synthesis, Biological Evaluation, ADME Prediction and Molecular Docking Studies

Jiqing Ye ^a, Xiao Yang ^b, Min Xu ^c, Paul Kay-sheung Chan ^{*b,d}, Cong Ma ^{*a}

^a State Key Laboratory of Chemical Biology and Drug Discovery, and Department of Applied Biology and Chemical Technology, The Hong Kong Polytechnic University, Kowloon, Hong Kong SAR

^b Department of Microbiology, The Chinese University of Hong Kong, Prince of Wales Hospital, Shatin, Hong Kong SAR

^c School of Electrical and Data Engineering, Faculty of Engineering and IT, University of Technology Sydney, Sydney, Australia

^d Stanley Ho Centre for Emerging Infectious Diseases, The Chinese University of Hong Kong, Shatin, Hong Kong SAR

Abstract

The discovery of novel potent neuraminidase (NA) inhibitors remains an attractive approach for treating infectious diseases caused by influenza. In this study, we describe the design and synthesis of novel *N*-substituted oseltamivir derivatives for probing the 150-cavity which is nascent to the activity site of NA. NA inhibitory studies showed

* Corresponding author, E-mail: cong.ma@polyu.edu.hk (C.M.) and paulkschan@cuhk.edu.hk (P.K.S.C.)

that new derivatives demonstrated the inhibitory activity with IC_{50} values at nM level against NA of a clinical influenza virus strain. Moreover, the *in silico* ADME predictions showed that the selected compounds had comparable properties with oseltamivir carboxylate, which demonstrated the druggability of these derivatives. Furthermore, molecular docking studies showed the most potent compound **6f** and **10i** adopt different modes of interaction with NA, which may provide novel solutions for treating oseltamivir-resistant influenza. Based on the research results, we consider that compounds **6f** and **10i** have the potential for further studies as novel antiviral agents.

Key words: Oseltamivir, derivative, Neuraminidase, 150-cavity, Influenza virus

1. Introduction

Influenza, commonly known as flu virus, represents a severe viral infection which can outbreak to become epidemic and even pandemic with elevated mortality rate [1]. Influenza viruses are unique among the viruses with regard to their antigenic variability, seasonality, and impact on the general population [2]. The continual emergence of new strains of influenza virus presents an ongoing threat to the global health and economic system. In the three types of influenza viruses (A, B and C) according to the serological reactivity of internal protein, influenza A caused more of the serious respiratory illness in humans [3]. While amongst influenza viruses of 18 hemagglutinin (HA) subtypes (H1 – 18) and 11 neuraminidase (NA) types (N1 – N11), influenza virus A subtype H3N2 (A/H3N2) is the most dominant flu strain infecting people associated with complications according to a report of the Centers for Disease Control and Prevention (CDC) [4], which caused one million death throughout the world in the Hong Kong Flu pandemic in 1968-1969 [5], and generates the current seasonal flu worldwide every year since 2004 [6]. Additionally, most A/H3N2 viruses contain genes from human, swine and avian viruses that demonstrated the possibility of cross-species infections evidenced by the Fujian flu epidemic in 2003 – 2004 [7], while the endemic of H3N2 in certain swine farms in China indicates the threat for emergence of future epidemics [8].

NA inhibitors (NAIs) can prevent nascent viruses infecting intact cells by inhibiting their release from host cells. The most successful NAIs include oseltamivir phosphate (**1**, ethyl ester prodrug) for oral administration [9], zanamivir (**2**) for

inhalation [10], Laninamivir (3) [11], and peramivir (4) [12] (Fig. 1). However, various NA mutants with resistance to oseltamivir have been identified in clinics. This is because some of the amino acids of NA must undergo a conformational change to accommodate the hydrophobic side chain of oseltamivir when the latter binds to the NA active site. A report showed that three sets of mutations (Arg292Lys, Asn294Ser, and His274Tyr) were able to prevent this conformational arrangement, and the presence of any of these mutants resulted in oseltamivir resistance [13]. Thus, there is an urgent need to discover novel oseltamivir derivatives for anti-influenza therapy.

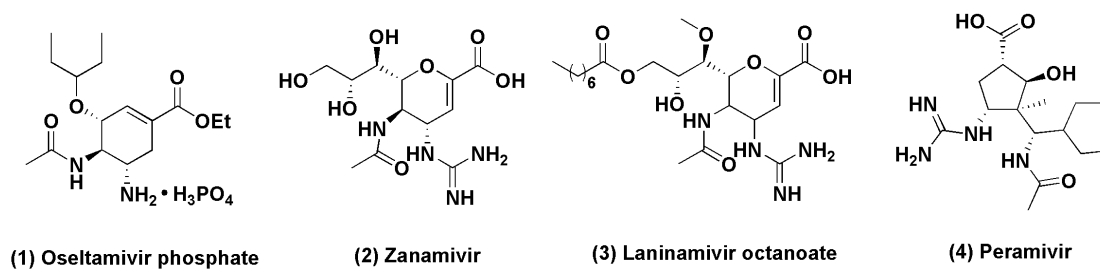


Fig. 1. Structures of the marketed NA inhibitors.

In 2006, Russell *et al.* determined the crystal structures of NAs from the N1, N4 and found that a loop of amino acids consisting of residues 147–152 (also known as the 150-loop or 150-cavity) together with the active site residues Asp151 and Glu119, adopted an open conformation [14]. A report demonstrated that the cavity opening of N2 NA could also be induced by the binding of oseltamivir carboxylate (OC, active drug after ester hydrolysis) to NA [15] (Fig. 3). These findings provided an opportunity for the *de novo* design of oseltamivir derivatives. In literature, the modifications on OC mostly focused on the derivatization at C-5-NH₂ of OC such as compounds (5) – (9)

[16-18], and the introduction of a triazole side chain at the C-6 position as shown in compounds (10) and (11) has also been described [19]. In addition, some OC derivatives such as compound (12) with a triazole ring incorporating the nitrogen at C-5 position and the double bond migrated towards the C-6 position have been reported [20] (Fig. 2). Results suggested that these derivatives might be capable of interacting with NA additionally through the 150-cavity, despite some of them lacking selectivity or structural data.

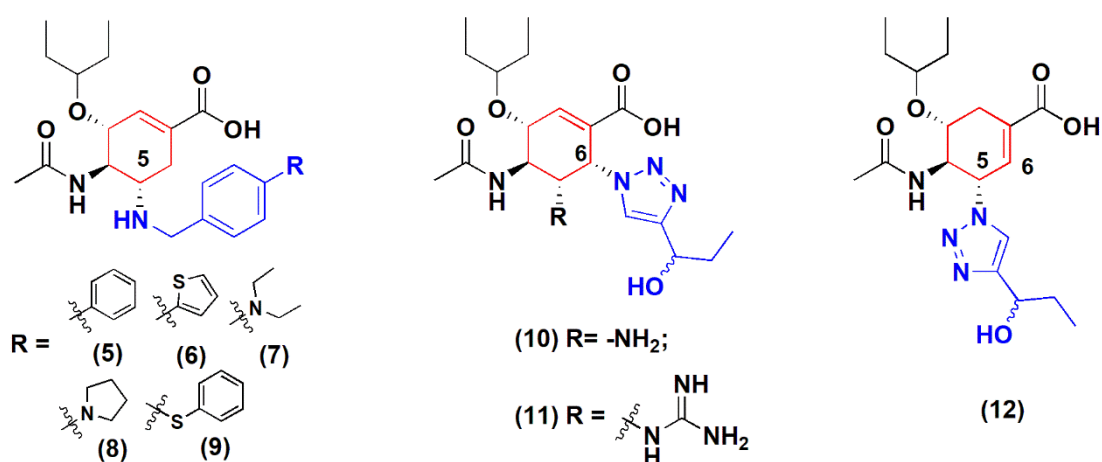


Fig. 2. OC derivatives reported in literature for probing the 150-cavity.

In this study, we planned to modify the C-5 amino group of OC, and several derivatives were designed, synthesized and evaluated the inhibitory activity of NA of a clinical A/H3N2 strain isolated from Hong Kong, as which is more valid to represent the real epidemic situation. Further *in silico* ADME predictions showed that the derivatives have comparable pharmacokinetic and pharmacodynamic properties with OC.

2. Results and discussion

2.1. Design of Oseltamivir derivatives

Our main objective in this research was to develop new NA inhibitors by targeting the 150-cavity. According to the docking model of **OC** to the active center of NA, C-5-NH₂ is very close to the 150-cavity. Liu *et al.* reported a series of oseltamivir derivatives bearing substituted benzyl amines at C-5 position [16-18]. While M2 channel blockers represent another class of successful anti-influenza drugs, such as amantadine and rimantadine [21], and recently, Wang *et al.* have reported a series of M2-S31 proton channel inhibitors with a general structure of adamantly-1-NH₂⁺CH₂-heteroaryl compounds [22-24] (**Fig. 3**). This inspired us to synthesize novel oseltamivir C-5-NH₂ substituted derivatives as anti-influenza agents (**Fig. 3**) by adapting the bioactive heteroaryl groups to substitute the C-5-NH₂ of **OC**. These modifications were used in this study for probing the 150-cavity and supposed to maintain the inhibitory activity and pharmacokinetic properties.

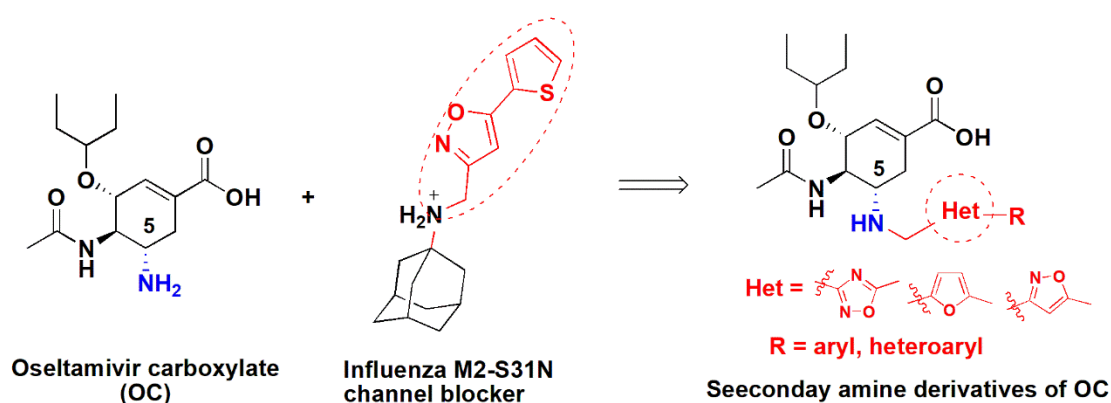
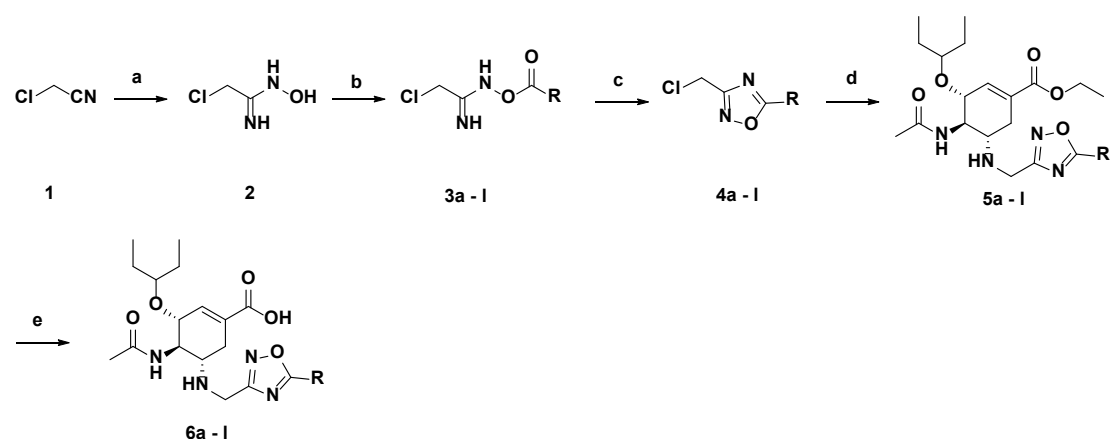


Fig. 3. Design of the new oseltamivir derivatives inspired by heteroaryl M2 channel blockers

2.2. Chemistry

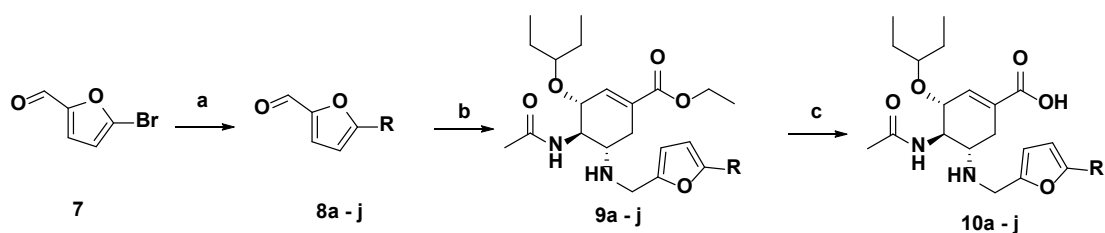
The synthesis of compounds **6a – I** bearing 1,2,4-oxadiazole are shown in **Scheme 1**. 2-chloro-*N*-hydroxyacetimidamide **2** was prepared from 2-chloroacetonitrile **1** and hydroxylamine. Condensation of various aryl chlorides with **2** gave the hydroxylamine esters **3a – I**. These esters cyclized to form the chloromethyl oxadiazole **4a – I**, then the chloride group was substituted by the C-5 amine of **OP** in the presence of *N,N*-diisopropylethylamine (DIPEA) to give **5a – I**. The hydrolysis of ethyl ester using sodium hydroxide (NaOH) provided acids **6a – I**.



Scheme 1. Synthetic route of compounds **6a – I**. Reagents and conditions: a) $\text{NH}_2\text{OH}\cdot\text{HCl}$, Na_2CO_3 , H_2O , r.t., 35 %; b) RC(O)Cl , K_2CO_3 , acetone, r.t., 88 %; c) AcOH , 120°C , 60 ~ 80 %; d) Oseltamivir phosphate, DIPEA, DMF, 70°C , 40 % ~ 70 %; e) NaOH , $\text{MeOH}/\text{H}_2\text{O}$, 50°C , 30 % ~ 50 %.

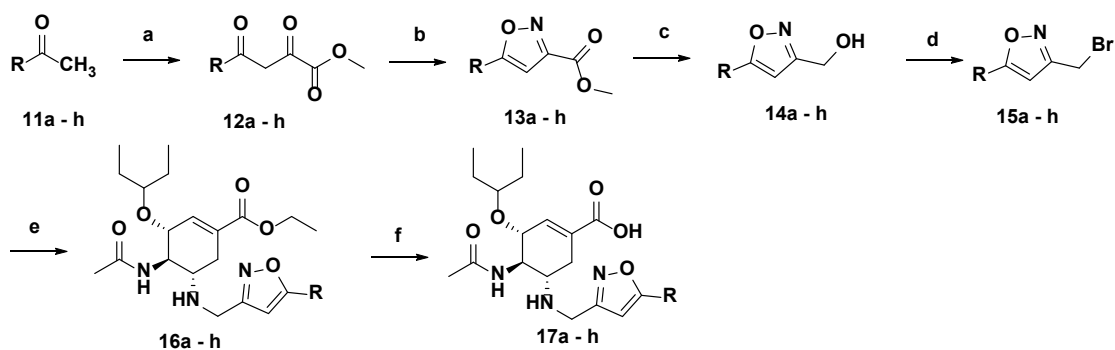
The synthesis of compounds **10a – j** with the furan scaffold is depicted in **Scheme 2**. Suzuki coupling of 5-bromofuran-2-carbaldehyde **7** with various boric acids furnished aldehydes **8a – j** with 50 % - 90 % overall yields. Reductive amination of **8a – j** using sodium triacetoxyborohydride ($\text{NaBH}(\text{OAc})_3$) provided amines **9a – j** with the overall

yields of 40 % - 60 %. After hydrolysis, the desired compounds **10a – j** were obtained.



Scheme 2. Synthesis of compounds **10a – j**. Reagents and conditions: a) $R_2B(OH)_2$, $Pd(dppf)_2Cl_2$, Na_2CO_3 , Tol/EtOH/ H_2O , $110^\circ C$, 50 % ~ 90 %; b) Oseltamivir phosphate, $NaBH(OAc)_3$, EtOH; 40 % ~ 60 %; c) NaOH, MeOH/ H_2O , $50^\circ C$, 30 % ~ 50 %.

The synthesis of compounds **17a – h** with the isoxazole scaffold is outlined in **Scheme 3**. Condensation of dimethyl oxalate with methyl ketones **11a – h** using potassium *tert*-butoxide as the base to afford intermediates **12a – h**, which cyclized with hydroxylamine hydrochloride at $50^\circ C$ in methanol to give the isoxazole ester intermediates **13a – h** with overall yields of 50 % - 80 %. The esters were reduced to provide alcohols **14a – h** by sodium borohydride and then converted to bromides **15a – h** by Appel-Lee reaction. The yields of these two steps ranged from 30 % - 60 %. Finally, a substitution reaction of bromides by C-5- NH_2 of oseltamivir was performed at $70^\circ C$ in DMF with DIPEA to provide **16a – h**, which were hydrolyzed to afford the desired products **17a – h**.



Scheme 3. Synthetic route of compounds **17a - h**. Reagents and conditions: a) Dimethyl oxalate, t-BuOK, Tol, r.t.; b) NH₂OH·HCl, MeOH, 50°C, 50 % ~ 80 %; c) NaBH₄, MeOH, reflux, 60 % ~ 75 %; d) CBr₄, PPh₃, CH₂Cl₂, 50 % ~ 60 %; e) Oseltamivir phosphate, DIPEA, DMF, 70°C, 40 % ~ 70 %; f) NaOH, MeOH/H₂O, 50°C, 30 % ~ 60 %.

2.3. Neuraminidase enzyme inhibitory assay

All the newly synthesized compounds were preliminarily screened for NA-inhibitory activity using MUNANA (4-(methylumbelliferyl)-N-acetylneuraminic acid) as the substrate of NA [25]. As mentioned above, a clinical A/H3N2 strain from Hong Kong was chosen and **OC** employed as the reference. **Table 1** showed the tested inhibitory potencies of the designed compounds at 1 nM.

Amongst the first series of **OC** derivatives (**6a - l**) with 1,2,4-oxadiazole substituted at C-5 amine, most of the compounds displayed the NA inhibitory activity at 1 nM, in which **6b** with a 4-CF₃ phenyl, **6d** with a pyridine-2-yl, **6e** with a 3-nitro phenyl, and **6f** with a furan-2-yl group demonstrated the significant activity with percentages of inhibition ≥ 10 %. Interestingly, **6a** with a thiophen-2-yl didn't show any activity, which differed from **6f** with one atom (S and O). The results suggested the size of the group at the C-5-NH-1,2,4-oxadiazole terminal position of **OC** was important for binding.

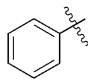
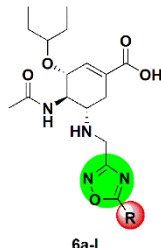
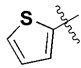
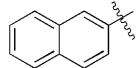
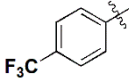
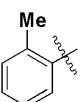
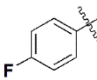
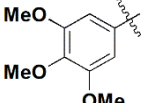
For compounds **10i - j**, all the substitutions at the C-5-NH-furanyl terminal position exhibited the inhibitory activity. While the electron-donating substituents such

as **10a**, **10e**, **10g** and **10i** respectively possessing 4-methoxyphenyl, 3,4-dimethoxyphenyl, thiophen-3-yl and 3,5-dimethylisoxazol-4-yl demonstrated the significant activity with percentages of inhibition > 10 %.

Lastly, all the C-5-NH-isoxazole derivatives **17a – j** showed mild inhibitory activity against NA at 1 nM regardless the electronic effects of substituents, compared to the other two series of compounds (**Table 1**).

In summary, most of our compounds possess the inhibitory activity against a clinically isolated of A/H3N2 NA. Particularly, **6f** and **10i** respectively bearing 5-(furan-2-yl)-1,2,4-oxadiazol-3-yl and 3,5-dimethylisoxazol-4-yl)furan-2-yl exhibited ~ 30 % of inhibition at 1 nM. Therefore, we further assessed the IC₅₀ values of compounds **6f** and **10i** (**Table 2**). Results showed that both compounds have very good inhibitory activity against the A/H3N2 influenza NA of a clinical sample, with IC₅₀ values of 1.92 ± 0.24 nM and 1.63 ± 0.16 nM, respectively (**Table 2**).

Table 1. Inhibition rate of designed compounds (1 nM) against a clinically isolated A/H3N2 influenza NA.

Derivatives	Cmpd.	R	% Inhibition ^a	Cmpd.	R	% Inhibition ^a
	OC	/	66.8 ± 0.4	6g		0.0 ± 2.0
 6a-l	6a		0.0 ± 2.2	6h		1.5 ± 1.2
	6b		8.0 ± 1.7	6i		0.5 ± 2.0
	6c		0.0 ± 3.5	6j		3.5 ± 3.1

6d		17.1 ± 2.0	6k		4.0 ± 5.9
6e		18.4 ± 3.6	6l		0.0 ± 2.6
6f		28.1 ± 1.7			
10a		14.7 ± 4.4	10f		5.5 ± 2.4
10b		3.2 ± 3.7	10g		12.5 ± 2.3
10c		8.4 ± 1.8	10h		4.8 ± 1.1
10d		3.7 ± 3.8	10i		30.2 ± 1.5
10e		12.9 ± 1.2	10j		10.9 ± 0.7
17a		1.6 ± 0.4	17e		8.1 ± 2.3
17b		5.2 ± 0.9	17f		0.4 ± 1.6
17c		3.9 ± 3.6	17g		3.0 ± 0.7
17d		5.4 ± 3.8	17h		0.3 ± 2.0

^a The data were the mean of the three independent experiments. % Inhibition =

$$\frac{(A_x - A_{bg}) - (A_0 - A_{bg})}{A_0 - A_{bg}} \times 100\%$$

A_0 is the absorbance of the control (no drug control), A_{bg} is the absorbance of the background, A_x is the absorbance of the sample or **OC**.

Table 2. Inhibitory activity of **6f** and **10i** against a clinically isolated A/H3N2 influenza NA (IC₅₀, nM)^a.

Compound	OC	6f	10i
IC ₅₀	0.11 ± 0.01	1.92 ± 0.24	1.63 ± 0.16

^a IC₅₀ is the compound concentration producing 50 % inhibition of NA, the values are the mean of three independent experiments.

2.4. *In silico* ADME evaluation

Computational calculation to predict absorption, distribution, metabolism and excretion (ADME) was used in the evaluation the drug-like properties of synthesized compounds [26-27]. Various pharmacokinetic and pharmacodynamic parameters of four compounds (**6d**, **6e**, **6f** and **10i**) with the greatest inhibitory activity in this research were calculated such as octanol-water partitioning coefficient (QPlogPo/w), aqueous solubility (QPlogS), binding to human serum albumin (QPlogKhsa), brain/blood partition coefficient (QPlogBB), number of likely metabolic reactions (#metab), central nervous system activity (CNS), predicted IC₅₀ value for blockage of HERG K⁺ channels (QPlogHERG), apparent Caco-2 cell permeability (QPPCaco), apparent MDCK cell permeability (QPPMDCK), and human oral absorption (**Table 3**).

As shown in **Table 3**, compared to **OC**, the synthetic derivatives have higher lipophilicity, and lower aqueous solubility. These results could be reasoned out because of the substitutions of C-5 amine group. Nevertheless, lipophilicity and solubility of the

derivatives were still drug-like. Moreover, the synthetic derivatives were suggested to bind slightly better to human serum albumin (**OC** < **6f** < **6d** < **6e** < **10i**) which indicated that more derivatives are required for the first dose if used *in vivo*. Furthermore, QPlogBB, CNS, #metab, QPlogHERG were well within the standard ranges. These results indicated that the derivatives should possess very low central nervous and heart toxicity with good metabolic stability. Clinical using anti-influenza drug oseltamivir phosphate is an ester prodrug of **OC** because of the poor absorptivity of the latter. This was consistent with our predicted results that both **OC** and its derivatives had quite poor permeability of Caco-2 and MDCK cells, which can be transformed to ester prodrugs to resolve this problem.

Table 3. Compliance of **OC** derivatives with the standard ranges of computational pharmacokinetic parameters (ADME).

Principal descriptors	OC	6d	6e	6f	10i	Standard Range ^a
QPlogPo/w	-1.654	-0.472	-0.692	-0.555	0.407	-2.0 - 6.5
QPlogS	-1.164	-3.549	-4.143	-3.135	-3.732	-6.5 - 0.5
QPlogKhsa	-0.873	-0.659	-0.538	-0.692	-0.236	-1.5 - 1.5
QPlogBB	-1.05	-1.741	-2.936	-1.55	-1.465	-3.0 - 1.2
#metab	3	5	5	5	7	1 - 8
CNS	-2	-2	-2	-2	-2	-2 (inactivity), +2 (activity)
QPlogHERG	-1.322	-3.575	-3.690	-3.236	-2.591	< -5
QPPCaco	7.34	5.374	0.749	6.759	6.731	< 25 poor, > 500 great
QPPMDCK	6.146	3.876	0.461	5.006	4.841	< 25 poor, > 500 great
(%) Human Oral Absorption	32.756	37.254	7.688	38.548	44.147	< 25 % is poor, > 80 % is high

Human Oral Absorption	Middle	Middle	Low	Middle	Middle
------------------------------	--------	--------	-----	--------	--------

^a Statistics of 95 % of known drugs according to Qikprop (Schrödiner[®] 2018).

2.4. Molecular docking model analysis of compound **6f** and **10i** with NA

The potential binding mode and key interactions of compounds **6f** and **10i** with NA were analyzed using Glide of Schrödiner[®]2018. As shown in **Fig. 4A**, though **6f** and **10i** are structurally very similar, it was demonstrated that these two compounds bound with the enzyme in different modes. The oseltamivir core fragment of compound **6f** occupied the active site in a similar manner to the binding pattern of **OC** while the 5-(furan-2-yl)-1,2,4-oxadiazole fragment stretched into the 150-cavity as desired. In **Fig. 4B**, it was suggested that **6f** retained the interactions of carboxyl acid with three residues (Arg118, Arg292 and Arg371) and acetamide on the C-4 position with Arg152. The C-5-NH formed one hydrogen bond with Asp151. Most of the residues around the heteroaromatic fragment were hydrophobic, such as Gly147, Trp438, Val116 (**Fig. S1**). In addition, **6f** made a directly interaction with Gln136 by H-bond. The docking model also explained why the inhibitory activity of **6f** was significant, while **6a** contains a sulfur atom which may not be able to fit into the 150-cavity.

Nevertheless, the pattern of interaction of **10i** with NA was suggested to be distinct from **OC** or **6f**. Indeed, **10i** was docked for binding to NA by overturning the molecule to prolong the 1-ethylpropoxy group into the inside area of enzyme, while the 3,5-dimethylisoxazol-4-yl group took over where the 1-ethylpropoxy group of **OC** occupies. As shown in **Fig. 4C**, the interactions would be formed between the carboxylic acid of

10i and Arg118 and Arg371, as well as acetamide at the C-4 position and Ser246. This type of docking model demonstrated less interactions with the enzyme when compared to **6f** or **OC** (**Fig. S1**). Note that the electron-donating groups substituted at C-5-NH-furanyl were favored for the inhibitory activity, which may be explained by the improved H-bond interactions of acetamide with NA.

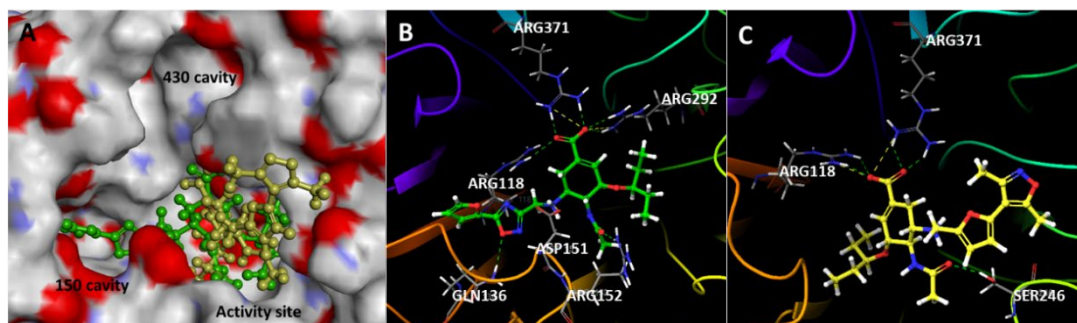


Fig. 4. (A) Binding modes of compounds **6f** (green) and **10i** (yellow) with NA (PDB 2HU0). Details of H-bond interactions of **6f** (B) and **10i** (C).

3. Conclusions

In this study, based on the crystal structure of NA and combination principle of drug design, we have designed, synthesized and evaluated the inhibitory activity of *N*-substituted oseltamivir derivatives containing C-5-NHCH₂-Aryl fragments. Four of the synthesized compounds, **6d**, **6e**, **6f** and **10i**, showed potent inhibitory activity (> 10 %) against NA at 1.0 nM. Among which, **6f** and **10i** were determined to be the most potent inhibitors against A/H3N2 NA of a clinical sample with IC₅₀ values of 1.92 ± 0.24 and 1.63 ± 0.16 nM, respectively. Further *in silico* ADME predictions showed that the pharmacokinetic and pharmacodynamic parameters of the selected compounds were all comparable to **OC** which suggested the druggability of these derivatives. Molecular docking studies of compound **6f** and **10i** have been performed, and the results showed that **6f** and **10i** adopted different modes of interaction with the NA, in which **6f** recruited the extra 150-cavity of the **OC**-NA binding site as designed. Therefore, further studies on the optimal binding with NA by employing the 150-cavity is worthwhile. While the conformation of **10i** was demonstrated to turn over to display a totally novel binding mode with NA with the 1-ethylpropoxy group extend into the inside of NA. As 1-ethylpropoxy was the problematic group causing the oseltamivir-resistance in influenza viruses, the structural diversification and optimization based on **10i** may provide new solutions of anti-influenza therapy.

4. Experimental section

4.1 Biology

4.1.1 NA enzyme inhibitory assay

The NA inhibition assay was performed using the commercially available NA-Fluor™ Influenza Neuraminidase Assay Kit. The substrate, MUNANA (4-(methylumbelliferyl)-N-acetylneuraminic acid) was cleaved by NA to yield a quantifiable fluorescent product. The tested compounds were dissolved in DMSO and diluted by the 1 × assay buffer (66.6 mM 2-(N-morpholino)ethanesulfonic acid (MES) buffer, 8 mM CaCl₂, pH 6.5) to 4 × the desired concentrations. In a 96-well plate, 25 μL of the 4 × compounds solution, 25 μL of the diluted virus sample were added and incubated for 20 to 30 min at 37°C. 50 μL of diluted 200 μM NA-Fluro™ Substrate working solution was added to each well and incubated for 60 min at 37°C. Finally, the reaction was terminated by adding 100 μL of NA-Fluor™ Stop Solution (0.2 M Na₂CO₃) and the fluorescence was read at an excitation wavelength of 350 nm and an emission of 460 nm.

4.2. Chemistry

4.2.1 General methods

Starting materials and reagents, unless otherwise stated, were of commercial grade and were used without further purification. All reactions were monitored by thin-layer chromatography (TLC) on glass sheets (Silica gel F₂₅₄) which can be visualized under UV light. Flash chromatography was carried out using silica gel (200-300 mesh). ¹H NMR (400 MHz) and ¹³C NMR (100 MHz) spectra were measured on BRUKER

AVANCE-III spectrometer. Chemical shifts are expressed in δ (ppm) and coupling constants (J) in Hz. The solvents for NMR were DMSO- d_6 (δ 2.5 for ^1H). High resolution MS spectra were measured using a QTOF-2 micromass Spectrometer by electron spray ionization.

4.2.2. 2-chloro-*N*-hydroxyacetimidamide (**2**)

A round bottom flask was charged a magnetic stirring, chloroacetonitrile (132 mmol, 10 g), hydroxylamine (9.2 g, 132 mmol) and 100 ml water in ice bath. Na_2CO_3 was added portion wise to the mixture, then warm to room temperature. After 2 h, sodium chloride aqueous solution was added, extracted with Et_2O , combined organic phase, washed by NaCl solution and filtered, the filtration was evaporated, and the residue was dried *in vacuo* to provide the titled compound as white solid, 5 g, 35 % yield.

4.2.3. General procedure for the synthesis of compound **3a – I**

To a solution of compound **2a** (1 eq.) in acetone was added acyl chloride dropwise at 0°C . Subsequently, the mixture was warmed to room temperature. After 4 h, the volatiles were removed *in vacuo* and the residue was partitioned between water and EA, the organic phase was washed with brine and dried with anhydrous Na_2SO_4 . The mixture was filtered, and the filtration was evaporated to afford crude product as pale-yellow solid.

4.2.4. General procedure for the synthesis of compound **4a – I**

Compound (**3a – I**) and acetic acid were added to a round bottom flask and heated to reflux. When TLC indicated that the reaction was completed, it was cooled to room

temperature and the solvents was removed in vacuum. NaHCO₃ aqueous solution was added to the residue, extracted by EA. The organic phase was combined and washed with brine and dried by anhydrous Na₂SO₄ and the crude mixture was evaporated and purified by column chromatography to provide the titled compound.

4.2.5. General procedure for the synthesis of compound **5a – l**

To a round-bottom flask were added Oseltamivir phosphate (1 eq), compound (**4a – l**) (1.2 eq.) and DMF. DIPEA (3 eq.) was added at room temperature and then heated to 70°C. After 12 h, water was added to the reaction mixture followed by extracting with EA. The combined organic phase was washed with NaCl solution, dried by Na₂SO₄ and evaporated to provide the titled compounds.

4.2.6. General procedure for the synthesis of compound **6a – l**

Compound (**5a – l**) (1 eq.) was dissolved in methanol and water (v: v = 5: 1), NaOH (5 eq.) was added. The reaction mixture was heated to 50°C overnight. Methanol was removed *in vacuo* and a small amount of water was added to the reaction mixture. The aqueous phase was washed by CH₂Cl₂ twice, then acidified to precipitate the target compounds.

4.2.7. (3*R*,4*R*,5*S*)-4-Acetamido-3-(pentan-3-yloxy)-5-(((5-(thiophen-2-yl)-1,2,4-oxadiazol-3-yl)methyl)amino)cyclohex-1-ene-1-carboxylic acid (**6a**)

Yield 38 %; white solid. ¹H NMR (400 MHz, DMSO) δ 8.08 (d, *J* = 4.8 Hz, 1H), 8.01 (d, *J* = 3.5 Hz, 1H), 7.75 (d, *J* = 9.0 Hz, 1H), 7.42 – 7.25 (m, 1H), 6.60 (s, 1H), 3.99 (d, *J* = 7.9 Hz, 1H), 3.87 (dd, *J* = 31.2, 15.1 Hz, 2H), 3.64 (dd, *J* = 18.7, 9.1 Hz, 1H), 3.35 – 3.30 (m, 2H), 2.79 – 2.65 (m, 2H), 1.85 – 2.06 (m, 1H), 1.84 (s, 3H), 1.35

– 1.45 (m, 4H), 0.83 (t, $J = 7.3$ Hz, 3H), 0.78 (t, $J = 7.4$ Hz, 3H). ^{13}C NMR (101 MHz, DMSO) δ 171.1, 170.2, 170.1, 168.1, 137.6, 134.2, 132.9, 129.8, 129.7, 125.2, 81.3, 75.7, 54.8, 54.6, 41.4, 30.9, 26.1, 25.6, 23.4, 9.9, 9.4. HRMS (ESI, m/z) calcd for $\text{C}_{21}\text{H}_{27}\text{N}_4\text{O}_5\text{S}$, 447.1708 [M-H⁻]; found, 447.1699.

4.2.8. *(3R,4R,5S)-4-Acetamido-3-(pentan-3-yloxy)-5-(((5-(4-(trifluoromethyl)phenyl)-1,2,4-oxadiazol-3-yl)methyl)amino)cyclohex-1-ene-1-carboxylic acid (6b)*

Yield 46 %; white solid. ^1H NMR (400 MHz, DMSO) δ 8.33 (d, $J = 8.1$ Hz, 2H), 8.02 (d, $J = 8.2$ Hz, 2H), 7.72 (d, $J = 8.9$ Hz, 1H), 6.38 (s, 1H), 3.93 (dd, $J = 34.1, 15.3$ Hz, 3H), 3.62 (d, $J = 9.1$ Hz, 2H), 3.30 (s, 1H), 2.72 (d, $J = 18.2$ Hz, 2H), 2.02 – 1.89 (m, 1H), 1.48 – 1.30 (m, 4H), 0.83 (t, $J = 7.3$ Hz, 3H), 0.77 (t, $J = 7.3$ Hz, 4H). ^{13}C NMR (101 MHz, DMSO) δ 174.2, 170.6, 170.2, 133.2, 132.9, 129.2, 127.7, 127.0 (q, $J = 3.6$ Hz), 125.4, 122.7, 81.1, 76.2, 55.0, 41.4, 39.7, 39.5, 39.3, 31.6, 26.2, 25.6, 23.5, 9.9, 9.4. HRMS (ESI, m/z) calcd for $\text{C}_{24}\text{H}_{28}\text{F}_3\text{N}_4\text{O}_5$, 509.2017 [M-H⁻]; found, 509.2009.

4.2.9. *(3R,4R,5S)-4-Acetamido-5-(((5-(4-fluorophenyl)-1,2,4-oxadiazol-3-yl)methyl)amino)-3-(pentan-3-yloxy)cyclohex-1-ene-1-carboxylic acid (6c)*

Yield 39 %; white solid. ^1H NMR (400 MHz, DMSO) δ 8.18 (dd, $J = 8.5, 5.4$ Hz, 2H), 7.76 (d, $J = 9.0$ Hz, 1H), 7.49 (t, $J = 8.8$ Hz, 2H), 6.60 (s, 1H), 3.99 (d, $J = 7.7$ Hz, 1H), 3.90 (dd, $J = 29.6, 15.2$ Hz, 2H), 3.65 (dd, $J = 18.2, 9.0$ Hz, 1H), 2.81 – 2.65 (m, 2H), 2.01 (dd, $J = 16.3, 8.7$ Hz, 1H), 1.40 (dd, $J = 11.6, 5.5$ Hz, 4H), 0.83 (t, $J = 7.3$ Hz, 3H), 0.78 (t, $J = 7.3$ Hz, 3H). ^{13}C NMR (101 MHz, DMSO) δ 174.5, 170.4, 170.1, 168.0, 165.4 (d, $J = 253.1$ Hz), 137.7, 131.1 (d, $J = 9.5$ Hz), 129.8, 120.8, 117.3 (d, $J = 22.5$ Hz), 81.3, 75.7, 54.7, 54.7, 41.5, 30.9, 26.1, 25.6, 23.5, 9.9, 9.4. HRMS (ESI, m/z) calcd

for C₂₃H₂₈N₄O₅, 459.2049 [M-H⁻]; found, 459.2035.

4.2.10. (3*R*,4*R*,5*S*)-4-Acetamido-3-(pentan-3-yloxy)-5-(((5-(pyridin-2-yl)-1,2,4-oxadiazol-3-yl)methyl)amino)cyclohex-1-ene-1-carboxylic acid (**6d**)

Yield 56 %; white solid. ¹H NMR (400 MHz, DMSO) δ 8.83 (d, *J* = 4.5 Hz, 1H), 8.26 (d, *J* = 7.8 Hz, 1H), 8.11 (td, *J* = 7.8, 1.5 Hz, 1H), 7.71 (dd, *J* = 7.1, 5.0 Hz, 1H), 7.66 (d, *J* = 16.5 Hz, 1H), 7.01 (s, 1H), 6.28 (s, 1H), 3.83 – 4.05 (m, 3H), 3.64 – 3.57 (m, 1H), 3.25 – 3.33 (m, 1H), 2.78 – 2.60 (m, 2H), 1.92 (dd, *J* = 17.5, 8.9 Hz, 1H), 1.82 (s, 3H), 1.44 – 1.33 (m, 4H), 0.83 (t, *J* = 7.3 Hz, 3H), 0.77 (t, *J* = 7.4 Hz, 3H). ¹³C NMR (101 MHz, DMSO) δ 174.4, 170.5, 170.1, 151.0, 143.5, 143.4, 138.6, 130.9, 127.8, 124.8, 80.9, 76.7, 55.3, 55.2, 41.5, 32.3, 26.2, 25.6, 23.5, 9.9, 9.4. HRMS (ESI, *m/z*) calcd for C₂₂H₂₈N₅O₅, 442.2096 [M-H⁻]; found, 442.2090.

4.2.11. (3*R*,4*R*,5*S*)-4-Acetamido-5-(((5-(3-nitrophenyl)-1,2,4-oxadiazol-3-yl)methyl)amino)-3-(pentan-3-yloxy)cyclohex-1-ene-1-carboxylic acid (**6e**)

Yield 66 %; white solid. ¹H NMR (400 MHz, DMSO) δ 8.80 (s, 1H), 8.61 – 8.47 (m, 2H), 7.97 (t, *J* = 7.9 Hz, 2H), 6.64 (s, 1H), 4.15 (d, *J* = 46.0 Hz, 3H), 3.80 (s, 1H), 3.28 – 2.91 (m, 2H), 2.81 (d, *J* = 15.5 Hz, 1H), 2.27 (s, 1H), 1.87 (s, 3H), 1.33 – 1.52 (m, 4H), 0.81 (dt, *J* = 20.5, 7.2 Hz, 6H). ¹³C NMR (101 MHz, DMSO) δ 174.0, 170.6, 167.7, 148.8, 137.9, 134.3, 132.1, 128.8, 128.2, 125.1, 122.9, 81.4, 75.2, 55.0, 53.3, 26.1, 25.6, 23.6, 9.9, 9.4. HRMS (ESI, *m/z*) calcd for C₂₃H₂₈N₅O₇, 486.1994 [M-H⁻]; found, 486.1985.

4.2.12. (3*R*,4*R*,5*S*)-4-Acetamido-5-(((5-(furan-2-yl)-1,2,4-oxadiazol-3-yl)methyl)amino)-3-(pentan-3-yloxy)cyclohex-1-ene-1-carboxylic acid (**6f**)

Yield 51 %; white solid. ^1H NMR (400 MHz, DMSO) δ 8.13 (s, 1H), 7.76 (d, $J = 8.9$ Hz, 1H), 7.55 (d, $J = 3.0$ Hz, 1H), 7.04 (s, 1H), 6.84 (s, 1H), 6.43 (s, 1H), 3.93 (s, 1H), 3.92 – 3.79 (m, 2H), 3.61 (d, $J = 9.0$ Hz, 1H), 3.30 (d, $J = 4.8$ Hz, 1H), 2.77 – 2.62 (m, 2H), 2.02 – 1.90 (m, 1H), 1.82 (s, 3H), 1.38 (s, 5H), 0.83 (d, $J = 6.9$ Hz, 3H), 0.76 (t, $J = 7.1$ Hz, 3H). ^{13}C NMR (101 MHz, DMSO) δ 170.2, 170.0, 169.7, 167.3, 148.6, 139.7, 133.9, 133.2, 117.7, 113.5, 81.1, 76.2, 55.1, 55.0, 41.3, 31.8, 26.2, 25.6, 23.4, 9.9, 9.4. HRMS (ESI, m/z) calcd for $\text{C}_{21}\text{H}_{27}\text{N}_4\text{O}_6$, 431.1936 $[\text{M}-\text{H}^-]$; found, 431.1930.

4.2.13. *(3R,4R,5S)-4-Acetamido-3-(pentan-3-yloxy)-5-(((5-phenyl-1,2,4-oxadiazol-3-yl)methyl)amino)cyclohex-1-ene-1-carboxylic acid (6g)*

Yield 49 %; white solid. ^1H NMR (400 MHz, DMSO) δ 8.12 (d, $J = 7.3$ Hz, 2H), 7.76 (d, $J = 9.1$ Hz, 1H), 7.71 (d, $J = 7.3$ Hz, 1H), 7.64 (t, $J = 7.5$ Hz, 2H), 7.04 (s, 1H), 6.54 (s, 1H), 3.91 (dd, $J = 32.1, 15.1$ Hz, 3H), 3.64 (d, $J = 9.3$ Hz, 1H), 3.33 – 3.30 (m, 1H), 2.73 (dd, $J = 17.6, 7.4$ Hz, 2H), 2.00 (dd, $J = 18.4, 10.7$ Hz, 1H), 1.83 (s, 3H), 1.47 – 1.28 (m, 4H), 0.82 (dd, $J = 14.4, 7.0$ Hz, 3H), 0.77 (d, $J = 7.4$ Hz, 3H). ^{13}C NMR (101 MHz, DMSO) δ 175.4, 170.4, 170.1, 168.7, 136.3, 133.6, 131.1, 130.0, 128.2, 124.0, 81.2, 75.9, 54.9, 54.8, 41.5, 31.2, 26.1, 25.6, 23.5, 9.9, 9.4. HRMS (ESI, m/z) calcd for $\text{C}_{23}\text{H}_{29}\text{N}_4\text{O}_5$, 441.2143 $[\text{M}-\text{H}^-]$; found, 441.2136.

4.2.14. *(3R,4R,5S)-4-Acetamido-5-(((5-(naphthalen-2-yl)-1,2,4-oxadiazol-3-yl)methyl)amino)-3-(pentan-3-yloxy)cyclohex-1-ene-1-carboxylic acid (6h)*

Yield 70 %, white solid. ^1H NMR (400 MHz, DMSO) δ 8.81 (s, 1H), 8.17 (dt, $J = 15.3, 8.2$ Hz, 3H), 8.06 (d, $J = 7.9$ Hz, 1H), 7.78 (d, $J = 9.0$ Hz, 1H), 7.75 – 7.64 (m, 2H), 6.62 (s, 1H), 4.00 (s, 1H), 3.95 (q, $J = 13.6$ Hz, 2H), 3.67 (dd, $J = 18.3, 9.2$ Hz,

1H), 2.85 – 2.70 (m, 2H), 2.04 (ddd, $J = 11.7, 8.1, 5.8$ Hz, 1H), 1.84 (s, 3H), 1.48 – 1.30 (m, 4H), 0.83 (t, $J = 7.3$ Hz, 3H), 0.78 (t, $J = 7.3$ Hz, 3H). ^{13}C NMR (101 MHz, DMSO) δ 175.5, 170.5, 170.2, 168.0, 137.9, 135.2, 132.8, 129.8, 129.7, 129.6, 129.4, 129.3, 128.4, 127.9, 124.0, 121.3, 81.3, 75.7, 54.8, 54.7, 41.6, 30.9, 26.1, 25.6, 23.5, 9.9, 9.4. HRMS (ESI, m/z) calcd for $\text{C}_{27}\text{H}_{31}\text{N}_4\text{O}_5$, 491.23 [M-H]⁻; found, 491.2288.

4.2.15. (3*R*,4*R*,5*S*)-4-Acetamido-3-(pentan-3-yloxy)-5-(((5-(*o*-tolyl)-1,2,4-oxadiazol-3-yl)methyl)amino)cyclohex-1-ene-1-carboxylic acid (**6i**)

Yield 69 %; white solid. ^1H NMR (400 MHz, DMSO) δ 8.04 (d, $J = 7.7$ Hz, 1H), 7.78 (d, $J = 9.1$ Hz, 1H), 7.57 (t, $J = 7.2$ Hz, 1H), 7.48 (d, $J = 7.6$ Hz, 1H), 7.44 (t, $J = 7.7$ Hz, 1H), 6.59 (s, 1H), 4.01 (s, 1H), 3.99 – 3.90 (m, 2H), 3.66 (d, $J = 9.4$ Hz, 1H), 3.33 (s, 1H), 2.83 – 2.69 (m, 2H), 2.65 (s, 3H), 2.02 (dd, $J = 17.0, 9.3$ Hz, 1H), 1.83 (s, 3H), 1.50 – 1.32 (m, 4H), 0.83 (t, $J = 7.4$ Hz, 3H), 0.78 (t, $J = 7.4$ Hz, 3H). ^{13}C NMR (101 MHz, DMSO) δ 175.9, 170.1, 169.9, 168.2, 138.9, 137.4, 133.0, 132.4, 130.2, 130.0, 127.1, 123.2, 81.3, 75.8, 54.8, 54.7, 41.5, 30.9, 26.1, 25.6, 23.4, 21.8, 9.9, 9.4. HRMS (ESI, m/z) calcd for $\text{C}_{24}\text{H}_{31}\text{N}_4\text{O}_5$, 455.23 [M-H]⁻; found, 455.2312.

4.2.16. (3*R*,4*R*,5*S*)-4-Acetamido-3-(pentan-3-yloxy)-5-(((5-(3,4,5-trimethoxyphenyl)-1,2,4-oxadiazol-3-yl)methyl)amino)cyclohex-1-ene-1-carboxylic acid (**6j**)

Yield 55 %; white solid. ^1H NMR (400 MHz, DMSO) δ 7.77 (d, $J = 9.0$ Hz, 1H), 7.38 (s, 2H), 6.59 (s, 1H), 3.99 (d, $J = 8.0$ Hz, 1H), 3.93 (d, $J = 15.3$ Hz, 2H), 3.89 (s, 6H), 3.77 (s, 3H), 3.66 (dd, $J = 18.8, 9.0$ Hz, 1H), 3.36 – 3.29 (m, 1H), 2.78 – 2.66 (m, 2H), 2.02 (dd, $J = 17.4, 9.3$ Hz, 1H), 1.85 (s, 3H), 1.33 – 1.50 (m, 4H), 0.83 (t, $J = 7.3$ Hz, 3H), 0.78 (t, $J = 7.4$ Hz, 3H). ^{13}C NMR (101 MHz, DMSO) δ 175.2, 170.4, 170.1,

168.1, 153.9, 142.0, 137.5, 130.0, 119.1, 105.6, 81.3, 75.7, 60.8, 56.7, 54.94, 54.6, 41.6, 31.0, 26.1, 25.6, 23.5, 9.9, 9.4. HRMS (ESI, m/z) calcd for C₂₆H₃₅N₄O₈, 531.246 [M-H⁻]; found, 531.2468.

4.2.17. *(3R,4R,5S)-4-Acetamido-5-(((5-(4-chlorophenyl)-1,2,4-oxadiazol-3-yl)methyl)amino)-3-(pentan-3-yloxy)cyclohex-1-ene-1-carboxylic acid (6k)*

Yield 39 %; white solid. ¹H NMR (400 MHz, DMSO) δ 8.13 (d, *J* = 6.7 Hz, 2H), 7.84 (s, 1H), 7.74 (d, *J* = 6.6 Hz, 2H), 6.63 (s, 1H), 4.04 (s, 3H), 3.73 (s, 1H), 2.92 (s, 1H), 2.76 (d, *J* = 17.1 Hz, 1H), 2.15 (s, 1H), 1.84 (s, 3H), 1.41 (s, 4H), 0.90 – 0.69 (m, 6H). ¹³C NMR (101 MHz, DMSO) δ 174.7, 170.4, 167.8, 138.7, 138.0, 136.0, 131.6, 130.3, 130.1, 129.2, 124.4, 122.7, 81.4, 75.5, 54.9, 54.0, 29.5, 26.1, 25.6, 23.6, 9.9, 9.4. HRMS (ESI, m/z) calcd for C₂₃H₂₈ClN₄O₅, 475.1754 [M-H⁻]; found, 475.1762.

4.2.18. *(3R,4R,5S)-4-acetamido-5-(((5-(2,6-difluorophenyl)-1,2,4-oxadiazol-3-yl)methyl)amino)-3-(pentan-3-yloxy)cyclohex-1-ene-1-carboxylic acid (6l)*

Yield 43 %; white solid. ¹H NMR (400 MHz, DMSO) δ 7.89 – 7.77 (m, 2H), 7.43 (t, *J* = 9.0 Hz, 2H), 6.62 (s, 1H), 4.11 – 3.93 (m, 3H), 3.69 (dd, *J* = 18.7, 9.1 Hz, 1H), 3.37 – 3.31 (m, 1H), 2.85 (s, 1H), 2.73 (dd, *J* = 17.4, 4.2 Hz, 1H), 2.08 (t, *J* = 12.2 Hz, 1H), 1.83 (s, 3H), 1.49 – 1.35 (m, 4H), 0.83 (t, *J* = 7.3 Hz, 3H), 0.78 (t, *J* = 7.4 Hz, 3H). ¹³C NMR (101 MHz, DMSO) δ 170.2, 169.9, 168.2, 167.9, 160.5 (d, *J* = 259.2 Hz), 160.3 (d, *J* = 259.4 Hz), 138.0, 136.3 (d, *J* = 11.1 Hz), 129.4, 113.6 (d, *J* = 21.2 Hz), 113.5 (d, *J* = 21.2 Hz), 103.0 (d, *J* = 16.3 Hz), 81.3, 75.6, 54.8, 54.4, 41.3, 30.5, 26.1, 25.6, 23.4, 9.9, 9.4. HRMS (ESI, m/z) calcd for C₂₃H₂₇F₂N₄O₅, 477.1955 [M-H⁻]; found, 477.1965.

4.2.19. General procedure for the synthesis of compound **8a – h**

5-Bromofuran-2-carbaldehyde (175 mg, 1 mmol), boronic acid (1 mmol, 1 equiv), Pd(dppf)₂Cl₂.DCM (16 mg, 2 % equiv), Na₂CO₃ (318 mg, 3 mmol, 3 equiv) were added to a Shrenk flask with 6 ml of Toluene, 1.5 ml H₂O and 1.5 ml EtOH. The reaction mixture was charged with N₂ and heated at 110°C overnight. The solution was extracted with EtOAc and the combined extracts were dried over Na₂SO₄. Chromatographic purification gave the titled compounds.

4.2.20. General procedure for the synthesis of compound **9a – h**

To a solution of oseltamivir phosphate (123 mg, 0.3 mmol) and aldehyde (0.36 mmol, 1.2 equiv) in 10 ml ethanol, NaBH(OAc)₃ (318 mg, 1.5 mmol) was slowly added. The mixture was stirred at room temperature overnight and then concentrated. To the residue, 20 ml saturated NaHCO₃ solution was added, and the mixture was extracted with EtOAc. The combined extracts were dried over anhydrous Na₂SO₄ and purified by chromatograph to give the products.

4.2.21. General procedure for the synthesis of compound **10a – h**

Compound (**9a – h**) (1 eq.) was dissolved in methanol and water (v: v = 5: 1), NaOH (5 eq.) was added. The reaction mixture was heated to 50°C overnight. Methanol was removed *in vacuum* and a small amount of water was added to the reaction mixture. The aqueous phase was washed by CH₂Cl₂ twice, then acidified to precipitate the target compounds.

4.2.22. (3*R*,4*R*,5*S*)-4-Acetamido-5-(((5-(4-methoxyphenyl)furan-2-yl)methyl)amino)-3-(pentan-3-yloxy)cyclohex-1-ene-1-carboxylic acid (**10a**)

Yield 68 %; white solid. ^1H NMR (400 MHz, DMSO) δ 7.81 (d, $J = 9.0$ Hz, 1H), 7.59 (d, $J = 8.7$ Hz, 2H), 6.97 (d, $J = 8.7$ Hz, 2H), 6.68 (d, $J = 3.1$ Hz, 1H), 6.61 (s, 1H), 6.29 (d, $J = 3.1$ Hz, 1H), 4.00 (d, $J = 7.8$ Hz, 1H), 3.80 (d, $J = 18.1$ Hz, 4H), 3.74 – 3.63 (m, 2H), 3.34 (dt, $J = 10.7, 5.3$ Hz, 1H), 2.84 – 2.65 (m, 2H), 2.02 (dd, $J = 16.9, 9.2$ Hz, 1H), 1.85 (s, 3H), 1.33 – 1.52 (m, 4H), 0.73 – 0.89 (m, 6H). ^{13}C NMR (101 MHz, DMSO) δ 170.1, 168.1, 159.0, 154.0, 152.5, 137.8, 129.8, 125.1, 124.0, 114.7, 109.1, 105.0, 81.3, 75.8, 55.6, 54.7, 54.7, 43.2, 30.9, 26.1, 25.6, 23.5, 9.9, 9.4. HRMS (ESI, m/z) calcd for $\text{C}_{26}\text{H}_{33}\text{N}_2\text{O}_6$, 469.2344 [$\text{M}-\text{H}^-$]; found, 469.2350.

4.2.23. (3*R*,4*R*,5*S*)-4-Acetamido-5-(((5-(4-fluorophenyl)furan-2-yl)methyl)amino)-3-(pentan-3-yloxy)cyclohex-1-ene-1-carboxylic acid (**10b**)

Yield 59 %; white solid. ^1H NMR (400 MHz, DMSO) δ 7.81 (d, $J = 8.9$ Hz, 1H), 7.75 – 7.52 (m, 2H), 7.25 (t, $J = 8.5$ Hz, 2H), 6.83 (s, 1H), 6.60 (s, 1H), 6.33 (s, 1H), 3.99 (s, 1H), 3.77 (dd, $J = 36.1, 15.0$ Hz, 2H), 3.67 (d, $J = 9.2$ Hz, 1H), 3.34 (s, 1H), 2.73 (dd, $J = 23.4, 11.8$ Hz, 2H), 2.01 (dd, $J = 16.1, 9.2$ Hz, 1H), 1.85 (s, 3H), 1.40 (dd, $J = 11.0, 5.5$ Hz, 4H), 0.90 – 0.66 (m, 6H). ^{13}C NMR (101 MHz, DMSO) δ 170.1, 164.9 (d, $J = 245.1$ Hz), 155.0, 151.5, 137.6, 130.0, 127.7 (d, $J = 2.9$ Hz), 125.6 (d, $J = 8.1$ Hz), 116.2 (d, $J = 22.0$ Hz), 109.3, 106.7, 81.3, 75.8, 54.7, 43.2, 40.6, 40.4, 40.2, 40.0, 39.8, 39.6, 39.4, 31.0, 26.1, 25.6, 23.5, 9.9, 9.4. HRMS (ESI, m/z) calcd for $\text{C}_{25}\text{H}_{30}\text{FN}_2\text{O}_5$, 457.2144 [$\text{M}-\text{H}^-$]; found, 457.2152.

4.2.24. (3*R*,4*R*,5*S*)-4-Acetamido-3-(pentan-3-yloxy)-5-(((5-(*o*-tolyl)furan-2-yl)methyl)amino)cyclohex-1-ene-1-carboxylic acid (**10c**)

Yield 70 %; white solid. ^1H NMR (400 MHz, DMSO) δ 7.80 (d, $J = 9.0$ Hz, 1H),

7.64 (d, $J = 7.4$ Hz, 1H), 7.31 – 7.18 (m, 3H), 6.66 – 6.58 (m, 2H), 6.37 (d, $J = 3.0$ Hz, 1H), 4.01 (d, $J = 7.8$ Hz, 1H), 3.79 (dd, $J = 39.2, 14.8$ Hz, 2H), 3.68 (dd, $J = 18.7, 9.3$ Hz, 1H), 3.38 – 3.30 (m, 1H), 2.65 – 2.85 (m, 2H), 2.44 (s, 3H), 2.02 (dd, $J = 17.2, 9.1$ Hz, 1H), 1.85 (s, 3H), 1.33-1.50 (m, 4H), 0.84 (t, $J = 7.5$ Hz, 3H), 0.79 (t, $J = 7.4$ Hz, 3H). ^{13}C NMR (101 MHz, DMSO) δ 170.0, 168.2, 154.5, 151.9, 137.7, 134.1, 131.7, 130.2, 129.9, 127.7, 126.6, 126.5, 110.1, 109.0, 81.3, 75.8, 54.8, 54.7, 43.1, 30.9, 26.1, 25.6, 23.4, 22.1, 9.9, 9.4. HRMS (ESI, m/z) calcd for $\text{C}_{26}\text{H}_{33}\text{N}_2\text{O}_5$, 453.2395 [M-H^-]; found, 453.2404.

4.2.25. *(3R,4R,5S)-4-Acetamido-5-(((5-(3,5-difluorophenyl)furan-2-yl)methyl)amino)-3-(pentan-3-yloxy)cyclohex-1-ene-1-carboxylic acid (10d)*

Yield 61 %; white solid. ^1H NMR (400 MHz, DMSO) δ 7.79 (d, $J = 9.0$ Hz, 1H), 7.37 (d, $J = 6.9$ Hz, 2H), 7.10 (dd, $J = 18.8, 6.2$ Hz, 2H), 6.61 (s, 1H), 6.39 (d, $J = 2.9$ Hz, 1H), 4.01 (d, $J = 7.6$ Hz, 1H), 3.79 (dd, $J = 35.1, 15.0$ Hz, 2H), 3.67 (dd, $J = 18.3, 9.1$ Hz, 1H), 3.30 – 3.40 (m, 1H), 2.83 – 2.62 (m, 2H), 2.02 (dd, $J = 16.8, 9.1$ Hz, 1H), 1.86 (s, 3H), 1.33 – 1.50 (m, 4H), 0.90 – 0.74 (m, 6H). ^{13}C NMR (101 MHz, DMSO) δ 170.0, 168.1, 163.4 (d, $J = 245.9$ Hz), 163.3 (d, $J = 246.4$ Hz), 156.2, 150.1, 137.8, 134.2, 134.1, 134.0, 129.7, 109.7 (d, $J = 8.3$ Hz), 106.5 (d, $J = 27.5$ Hz), 102.6 (d, $J = 26.2$ Hz), 81.3, 75.7, 54.7, 54.6, 43.0, 30.8, 26.1, 25.6, 23.4, 9.9, 9.4. HRMS (ESI, m/z) calcd for $\text{C}_{25}\text{H}_{29}\text{F}_2\text{N}_2\text{O}_5$, 475.205 [M-H^-]; found, 475.2060.

4.2.26. *(3R,4R,5S)-4-Acetamido-5-(((5-(3,4-dimethoxyphenyl)furan-2-yl)methyl)amino)-3-(pentan-3-yloxy)cyclohex-1-ene-1-carboxylic acid (10e)*

Yield 66 %; white solid. ^1H NMR (400 MHz, DMSO) δ 7.98 (d, $J = 6.6$ Hz, 1H),

7.25 (s, 2H), 7.04 – 6.93 (m, 1H), 6.80 (d, $J = 2.7$ Hz, 1H), 6.65 (s, 1H), 6.51 (s, 1H), 3.95 – 4.22 (m, 3H), 3.86 (d, $J = 13.3$ Hz, 1H), 3.82 (s, 3H), 3.78 (s, 3H), 3.33 – 3.42 (m, 1H), 3.10 (s, 1H), 2.88 (d, $J = 16.5$ Hz, 1H), 2.35 (s, 1H), 1.89 (s, 3H), 1.48 – 1.36 (m, 4H), 0.77 – 0.89 (m, 6H). ^{13}C NMR (101 MHz, DMSO) δ 170.6, 167.6, 153.7, 149.6, 149.1, 138.0, 128.9, 123.8, 116.7, 112.7, 112.0, 108.0, 105.6, 81.5, 75.3, 56.1, 56.1, 54.5, 53.0, 41.3, 28.5, 26.1, 25.6, 23.7, 9.8, 9.3. HRMS (ESI, m/z) calcd for $\text{C}_{27}\text{H}_{35}\text{N}_2\text{O}_7$, 499.245 [M-H $^-$]; found, 499.2459.

4.2.27. *(3R,4R,5S)-4-Acetamido-5-(((5-(3-chlorophenyl)furan-2-yl)methyl)amino)-3-(pentan-3-yloxy)cyclohex-1-ene-1-carboxylic acid (10f)*

Yield 65 %; white solid. ^1H NMR (400 MHz, DMSO) δ 7.75 (d, $J = 8.8$ Hz, 1H), 7.70 (s, 1H), 7.62 (d, $J = 7.5$ Hz, 1H), 7.43 (t, $J = 7.8$ Hz, 1H), 7.30 (d, $J = 7.5$ Hz, 1H), 6.99 (d, $J = 2.0$ Hz, 1H), 6.34 (d, $J = 9.8$ Hz, 2H), 3.92 (d, $J = 6.4$ Hz, 1H), 3.77 (dd, $J = 47.8, 14.8$ Hz, 2H), 3.63 (dd, $J = 17.6, 8.8$ Hz, 1H), 3.31 (s, 1H), 2.70 (t, $J = 11.6$ Hz, 2H), 1.99 – 1.89 (m, 1H), 1.85 (s, 3H), 1.33-1.45 (m, 4H), 0.87 – 0.72 (m, 6H). ^{13}C NMR (101 MHz, DMSO) δ 170.0, 155.9, 150.7, 135.9, 134.17, 132.9, 131.2, 127.2, 123.1, 122.1, 109.4, 108.4, 80.9, 76.6, 55.3, 55.3, 43.2, 32.2, 26.2, 25.7, 23.5, 10.0, 9.5. HRMS (ESI, m/z) calcd for $\text{C}_{25}\text{H}_{30}\text{ClN}_2\text{O}_5$, 473.1849 [M-H $^-$]; found, 473.1861.

4.2.28. *(3R,4R,5S)-4-Acetamido-3-(pentan-3-yloxy)-5-(((5-(thiophen-3-yl)furan-2-yl)methyl)amino)cyclohex-1-ene-1-carboxylic acid (10g)*

Yield 55 %; white solid. ^1H NMR (400 MHz, DMSO) δ 7.80 (d, $J = 9.0$ Hz, 1H), 7.62 (s, 2H), 7.40 (dd, $J = 4.0, 1.9$ Hz, 1H), 6.64 (d, $J = 2.9$ Hz, 1H), 6.61 (s, 1H), 6.29 (d, $J = 2.8$ Hz, 1H), 4.01 (d, $J = 7.7$ Hz, 1H), 3.76 (dd, $J = 32.9, 11.8$ Hz, 2H), 3.70 –

3.63 (m, 1H), 3.36 – 3.33 (m, 1H), 2.74 (ddd, $J = 26.1, 15.8, 4.7$ Hz, 2H), 2.02 (dd, $J = 16.8, 9.4$ Hz, 1H), 1.85 (s, 3H), 1.33 – 1.50 (m, 4H), 0.87 – 0.75 (m, 6H). ^{13}C NMR (101 MHz, DMSO) δ 170.1, 168.1, 154.1, 149.8, 137.8, 132.8, 129.8, 127.7, 125.1, 119.0, 108.8, 106.4, 81.3, 75.8, 54.7, 43.2, 30.9, 26.1, 25.6, 23.5, 9.9, 9.4. HRMS (ESI, m/z) calcd for $\text{C}_{23}\text{H}_{29}\text{N}_2\text{O}_5\text{S}$, 445.1803 [M-H^-]; found, 445.1815.

4.2.29. *(3R,4R,5S)-4-acetamido-5-(((5-(5-chloro-2-methylphenyl)furan-2-yl)methyl)amino)-3-(pentan-3-yloxy)cyclohex-1-ene-1-carboxylic acid (10h)*

Yield 50 %; white solid. ^1H NMR (400 MHz, DMSO) δ 8.02 (s, 1H), 7.76 (s, 1H), 7.39 – 7.26 (m, 2H), 6.83 (d, $J = 2.6$ Hz, 1H), 6.65 (s, 2H), 4.16 (s, 3H), 3.87 (s, 1H), 3.38 (d, $J = 5.5$ Hz, 1H), 2.87 (d, $J = 16.2$ Hz, 1H), 2.50 (s, 3H), 2.44 (s, 3H), 1.90 (s, 3H), 1.50 – 1.35 (m, 4H), 0.84 (t, $J = 7.3$ Hz, 3H), 0.79 (t, $J = 7.4$ Hz, 3H). ^{13}C NMR (101 MHz, DMSO) δ 174.9, 170.8, 167.5, 151.6, 138.0, 133.6, 133.2, 131.4, 131.2, 128.6, 127.6, 126.1, 111.6, 81.5, 75.1, 54.4, 52.4, 29.5, 26.0, 25.5, 23.7, 21.5, 9.9, 9.3. HRMS (ESI, m/z) calcd for $\text{C}_{26}\text{H}_{32}\text{ClN}_2\text{O}_5$, 487.2005 [M-H^-]; found, 487.1988.

4.2.30. *(3R,4R,5S)-4-acetamido-5-(((5-(3,5-dimethylisoxazol-4-yl)furan-2-yl)methyl)amino)-3-(pentan-3-yloxy)cyclohex-1-ene-1-carboxylic acid (10i)*

Yield 66 %; white solid. ^1H NMR (400 MHz, DMSO) δ 7.86 (d, $J = 8.7$ Hz, 1H), 6.62 (s, 1H), 6.55 (d, $J = 3.0$ Hz, 1H), 6.45 (s, 1H), 4.04 (d, $J = 7.2$ Hz, 1H), 3.90 (d, $J = 11.4$ Hz, 2H), 3.72 (dd, $J = 18.1, 9.0$ Hz, 1H), 3.34 (d, $J = 5.5$ Hz, 1H), 2.88 (s, 1H), 2.82 – 2.71 (m, 1H), 2.50 (s, 3H), 2.34 (s, 3H), 2.21 – 2.04 (m, 1H), 1.85 (s, 3H), 1.47 – 1.34 (m, 4H), 0.83 (t, $J = 7.4$ Hz, 3H), 0.79 (t, $J = 7.4$ Hz, 3H). ^{13}C NMR (101 MHz, DMSO) δ 170.3, 167.9, 165.5, 157.6, 144.3, 138.0, 129.2, 109.8, 108.3, 108.2, 81.3,

75.6, 54.4, 54.0, 42.0, 31.2, 26.1, 25.6, 23.5, 12.5, 11.6, 9.9, 9.8, 9.4. HRMS (ESI, m/z) calcd for C₂₄H₃₂N₃O₆, 458.2297 [M-H⁻]; found, 458.2286.

4.2.31. *(3R,4R,5S)-4-acetamido-5-(((5-(dibenzo[b,d]furan-4-yl)furan-2-yl)methyl)amino)-3-(pentan-3-yloxy)cyclohex-1-ene-1-carboxylic acid (10j)*

Yield 81 %; white solid. ¹H NMR (400 MHz, DMSO) δ 8.20 (d, *J* = 7.6 Hz, 1H), 8.09 (d, *J* = 7.5 Hz, 1H), 7.97 – 7.76 (m, 3H), 7.58 (t, *J* = 7.6 Hz, 1H), 7.47 (dt, *J* = 12.5, 7.6 Hz, 2H), 7.27 (d, *J* = 2.8 Hz, 1H), 6.64 (s, 1H), 6.61 (s, 1H), 4.15 – 3.70 (m, 4H), 3.30 – 3.40 (m, 1H), 2.97 (s, 1H), 2.82 (d, *J* = 15.4 Hz, 1H), 2.31 – 2.10 (m, 1H), 1.89 (s, 3H), 1.41 (dt, *J* = 18.7, 6.8 Hz, 4H), 0.84 (t, *J* = 7.6 Hz, 3H), 0.79 (t, *J* = 7.5 Hz, 3H). ¹³C NMR (101 MHz, DMSO) δ 170.3, 167.9, 156.0, 151.0, 147.9, 138.0, 129.4, 128.4, 124.8, 123.9, 123.7, 122.4, 121.8, 120.3, 115.8, 112.4, 111.4, 81.4, 75.6, 54.7, 54.2, 42.5, 30.2, 26.1, 25.6, 23.6, 9.9, 9.4. HRMS (ESI, m/z) calcd for C₃₁H₃₃N₂O₆, 529.2344 [M-H⁻]; found, 529.2328.

4.2.32. *General procedure for the synthesis of compound 13a – h*

To a stirred solution of dimethyl oxalate (1.1 eq.) and methyl ketone (1 eq.) in toluene was added a solution of potassium tert-butoxide (1.2 eq.) in THF. The resulting solution was stirred at room temperature overnight. The reaction was quenched with 1 N HCl and extracted with ethyl acetate. The combined organic layers were dried over Na₂SO₄, filtered and concentrated under reduced pressure. The crude product (**12a – h**) was dissolved in methanol and hydroxylamine hydrochloride was added. The solution was heated to 50°C for 6 hrs. The solvents were removed under reduced pressure and the resulting isoxazole ester was purified by flash column chromatography to provide

the target compounds.

4.2.33. General procedure for the synthesis of compound 14a – h

Ester (1 eq.) was dissolved in methanol and cooled down to 0°C. NaBH₄ (4 eq.) was added in small portions to the solution over 10 min. The mixture was warmed slowly to 50°C and stirred for five hours. NH₄Cl aqueous solution was added and the organic solvent was removed under reduced pressure. The resulting aqueous layer was extracted with ethyl acetate (3 ×), and the organic layers were combined and dried over Na₂SO₄, and the solvents was removed under reduced pressure. This hydroxyl intermediate was used for the next step without further purification.

4.2.34. General procedure for the synthesis of compound 15a – h

Hydroxyl intermediate (1 eq.) was dissolved in DCM, and the resulting solution was cooled down to 0°C. CBr₄ (1.5 eq.) and PPh₃ (1.5 eq.) were added sequentially. The solution was stirred at 0°C for 30 min and gradually warmed up to room temperature. The solvent was removed to provide the intermediates (**15a – h**).

4.2.35. General procedure for the synthesis of compound 16a – h

To a round-bottom flask were added Oseltamivir phosphate (1 eq.), compound (**15a – h**) (1.2 eq.) and DMF. DIPEA (3 eq.) was added at r.t. and heated to 70°C. After 12 h, water was added to the reaction mixture followed by extracting with EA. The combined organic phase was washed with NaCl solution, dried by Na₂SO₄ and evaporated to provide the titled compounds.

4.2.36. General procedure for the synthesis of compound 17a – h

Compound (**16a – h**) (1 eq.) was dissolved in methanol and water (v: v = 5: 1),

NaOH (5 eq.) was added. The reaction mixture was heated to 50°C overnight. Methanol was removed *in vacuum* and a small amount of water was added to the reaction mixture. The aqueous phase was washed by CH₂Cl₂ twice, then acidified to precipitate the target compounds.

4.2.37. (3*R*,4*R*,5*S*)-4-Acetamido-3-(pentan-3-yloxy)-5-(((3-phenylisoxazol-5-yl)methyl)amino)cyclohex-1-ene-1-carboxylic acid (**17a**)

Yield 55 %; white solid. ¹H NMR (400 MHz, DMSO) δ 7.85 (d, *J* = 7.4 Hz, 2H), 7.79 (d, *J* = 9.0 Hz, 1H), 7.59 – 7.45 (m, 3H), 6.95 (s, 1H), 6.61 (s, 1H), 4.01 (d, *J* = 7.9 Hz, 1H), 3.84 (dd, *J* = 30.1, 14.6 Hz, 2H), 3.68 (dd, *J* = 18.4, 9.1 Hz, 1H), 3.34 (s, 1H), 2.71 (t, *J* = 14.0 Hz, 2H), 2.08 – 1.95 (m, 1H), 1.86 (s, 3H), 1.53 – 1.30 (m, 4H), 0.83 (t, *J* = 7.5 Hz, 3H), 0.79 (t, *J* = 7.5 Hz, 3H). ¹³C NMR (101 MHz, DMSO) δ 170.2, 169.1, 168.0, 164.6, 138.0, 130.7, 129.7, 129.5, 127.5, 126.0, 100.5, 81.3, 75.8, 54.7, 41.4, 30.8, 26.1, 25.6, 23.6, 9.9, 9.4. HRMS (ESI, *m/z*) calcd for C₂₄H₃₀N₃O₅, 440.2191 [M-H⁻]; found, 440.2173.

4.2.38. (3*R*,4*R*,5*S*)-4-Acetamido-5-(((3-(4-chlorophenyl)isoxazol-5-yl)methyl)amino)-3-(pentan-3-yloxy)cyclohex-1-ene-1-carboxylic acid (**17b**)

Yield 56 %; white solid. ¹H NMR (400 MHz, DMSO) δ 7.87 (d, *J* = 8.3 Hz, 2H), 7.80 (d, *J* = 9.0 Hz, 1H), 7.61 (d, *J* = 8.3 Hz, 2H), 7.00 (s, 1H), 6.60 (s, 1H), 4.00 (d, *J* = 7.3 Hz, 1H), 3.87 – 3.77 (m, 2H), 3.67 (d, *J* = 9.0 Hz, 1H), 3.33 (d, *J* = 5.1 Hz, 1H), 2.80 – 2.60 (m, 2H), 2.06 – 1.94 (m, 1H), 1.86 (s, 3H), 1.50 – 1.29 (m, 4H), 0.84 (t, *J* = 7.5 Hz, 3H), 0.79 (t, *J* = 7.5 Hz, 3H). ¹³C NMR (101 MHz, DMSO) δ 170.2, 168.1, 167.9, 164.9, 137.8, 135.3, 129.8, 127.8, 126.4, 101.1, 81.3, 75.8, 54.8, 54.7, 41.5, 30.9,

26.09, 25.6, 23.5, 9.9, 9.4. HRMS (ESI, m/z) calcd for C₂₄H₂₉N₃O₅, 474.1801 [M-H⁻]; found, 474.1785.

4.2.39. *(3R,4R,5S)-4-Acetamido-3-(pentan-3-yloxy)-5-(((3-(p-tolyl)isoxazol-5-yl)methyl)amino)cyclohex-1-ene-1-carboxylic acid (17c)*

Yield 35 %, white solid. ¹H NMR (400 MHz, DMSO) δ 7.87 (d, *J* = 8.9 Hz, 1H), 7.73 (d, *J* = 7.9 Hz, 2H), 7.34 (d, *J* = 7.9 Hz, 2H), 6.88 (s, 1H), 6.58 (s, 1H), 4.01 (d, *J* = 7.8 Hz, 1H), 3.80 (dd, *J* = 30.6, 14.7 Hz, 2H), 3.67 (d, *J* = 9.2 Hz, 1H), 3.35 – 3.32 (m, 1H), 2.76 – 2.60 (m, 2H), 2.36 (s, 3H), 1.99 (dd, *J* = 16.4, 8.8 Hz, 1H), 1.86 (s, 3H), 1.47 – 1.29 (m, 4H), 0.83 (t, *J* = 7.5 Hz, 3H), 0.79 (t, *J* = 7.4 Hz, 3H). ¹³C NMR (101 MHz, DMSO) δ 170.2, 169.2, 168.2, 164.7, 140.5, 137.5, 130.2, 130.1, 125.9, 124.9, 99.8, 81.3, 75.9, 54.8, 54.7, 41.5, 31.0, 26.1, 25.6, 23.5, 21.5, 9.9, 9.4. HRMS (ESI, m/z) calcd for C₂₅H₃₂N₃O₅, 454.2347 [M-H⁻]; found, 454.2332.

4.2.40. *(3R,4R,5S)-4-acetamido-5-(((3-(4-methoxyphenyl)isoxazol-5-yl)methyl)amino)-3-(pentan-3-yloxy)cyclohex-1-ene-1-carboxylic acid (17d)*

Yield 66 %; white solid. ¹H NMR (400 MHz, DMSO) δ 7.78 (d, *J* = 8.6 Hz, 3H), 7.08 (d, *J* = 8.7 Hz, 2H), 6.79 (s, 1H), 6.59 (s, 1H), 3.99 (d, *J* = 7.8 Hz, 1H), 3.87 – 3.72 (m, 5H), 3.66 (dd, *J* = 18.8, 9.2 Hz, 1H), 3.30 – 3.36 (m, 1H), 2.75 – 2.63 (m, 2H), 1.99 (dd, *J* = 16.5, 8.7 Hz, 1H), 1.86 (s, 3H), 1.33 – 1.46 (m, 4H), 0.83 (t, *J* = 7.4 Hz, 3H), 0.79 (t, *J* = 7.4 Hz, 3H). ¹³C NMR (101 MHz, DMSO) δ 170.1, 169.1, 168.2, 164.6, 161.2, 129.8, 127.7, 120.3, 115.1, 98.9, 81.3, 75.8, 55.8, 54.8, 54.7, 41.5, 31.0, 26.1, 25.6, 23.5, 9.9, 9.4. HRMS (ESI, m/z) calcd for C₂₅H₃₂N₃O₆, 470.2297 [M-H⁻]; found, 470.2279.

4.2.41. *(3R,4R,5S)-4-Acetamido-3-(pentan-3-yloxy)-5-(((3-(4-(trifluoromethyl)phenyl)isoxazol-5-yl)methyl)amino)cyclohex-1-ene-1-carboxylic acid (17e)*

Yield 50 %; white solid. ¹H NMR (400 MHz, DMSO) δ 8.08 (d, *J* = 8.0 Hz, 2H), 7.91 (d, *J* = 8.2 Hz, 2H), 7.83 (d, *J* = 9.1 Hz, 1H), 7.16 (s, 1H), 6.59 (s, 1H), 4.01 (d, *J* = 7.7 Hz, 1H), 3.85 (dd, *J* = 28.3, 14.7 Hz, 2H), 3.67 (dd, *J* = 18.3, 9.1 Hz, 1H), 3.35 – 3.32 (m, 1H), 2.63 – 2.78 (m, 2H), 2.01 (dd, *J* = 16.4, 9.0 Hz, 1H), 1.86 (s, 3H), 1.32 – 1.44 (m, 4H), 0.83 (t, *J* = 7.5 Hz, 3H), 0.79 (t, *J* = 7.5 Hz, 3H). ¹³C NMR (101 MHz, DMSO) δ 170.2, 168.2, 167.4, 165.1, 137.5, 131.1, 130.6, 130.3, 130.0, 128.5, 126.8, 126.7, 126.7, 126.6, 124.4 (q, *J* = 272.7 Hz), 102.4, 81.3, 75.9, 54.8, 41.5, 31.0, 26.1, 25.6, 23.5, 9.9, 9.4. HRMS (ESI, *m/z*) calcd for C₂₅H₂₉F₃N₃O₅, 508.2065 [M-H⁻]; found, 508.2049.

4.2.42. *(3R,4R,5S)-4-acetamido-5-(((3-(3,4-difluorophenyl)isoxazol-5-yl)methyl)amino)-3-(pentan-3-yloxy)cyclohex-1-ene-1-carboxylic acid (17f)*

Yield 51 %; white solid. ¹H NMR (400 MHz, DMSO) δ 8.05 – 7.92 (m, 1H), 7.81 (d, *J* = 8.3 Hz, 1H), 7.73 (s, 1H), 7.63 (dd, *J* = 18.8, 8.6 Hz, 1H), 7.03 (s, 1H), 6.59 (s, 1H), 3.99 (d, *J* = 8.0 Hz, 1H), 3.82 (q, *J* = 14.7 Hz, 2H), 3.67 (dd, *J* = 18.5, 9.2 Hz, 1H), 3.35 – 3.32 (m, 1H), 2.78 – 2.62 (m, 2H), 2.06 – 1.94 (m, 1H), 1.86 (s, 3H), 1.41 (qt, *J* = 13.7, 6.7 Hz, 4H), 0.81 (dt, *J* = 17.7, 7.3 Hz, 6H). ¹³C NMR (101 MHz, DMSO) δ 170.1, 168.2, 167.0, 165.1, 150.9 (dd, *J* = 263.6 Hz, 12.5 Hz), 150.3 (dd, *J* = 260.6 Hz, 13.1 Hz), 137.5, 130.0, 125.1, 125.0, 125.0, 125.0, 123.3, 119.2, 119.1, 115.6, 115.4, 101.5, 81.3, 75.8, 54.8, 54.7, 41.5, 31.0, 26.1, 25.6, 23.5, 9.9, 9.4. HRMS (ESI, *m/z*)

calcd for C₂₄H₂₈F₂N₃O₅, 476.2003 [M-H⁻]; found, 476.1994.

4.2.43. (3*R*,4*R*,5*S*)-4-acetamido-3-(pentan-3-yloxy)-5-(((3-(thiophen-2-yl)isoxazol-5-yl)methyl)amino)cyclohex-1-ene-1-carboxylic acid (**17g**)

Yield 37 %; white solid. ¹H NMR (400 MHz, DMSO) δ 7.99 (d, *J* = 4.6 Hz, 1H), 7.84 (d, *J* = 4.8 Hz, 1H), 7.71 (d, *J* = 3.2 Hz, 1H), 7.31 – 7.19 (m, 1H), 6.93 (s, 1H), 6.63 (s, 1H), 4.11 (s, 3H), 3.81 (d, *J* = 8.2 Hz, 1H), 3.39 – 3.35 (m, 1H), 3.10 (s, 1H), 2.80 (d, *J* = 15.5 Hz, 1H), 2.30 (s, 1H), 1.88 (s, 3H), 1.42 (qt, *J* = 13.7, 6.8 Hz, 4H), 0.83 (t, *J* = 7.3 Hz, 3H), 0.79 (t, *J* = 7.4 Hz, 3H). ¹³C NMR (101 MHz, DMSO) δ 170.7, 167.6, 164.8, 138.1, 130.1, 129.2, 128.7, 128.6, 128.4, 100.4, 81.5, 75.2, 54.7, 53.0, 28.5, 26.0, 25.5, 23.8, 9.9, 9.4. HRMS (ESI, *m/z*) calcd for C₂₂H₂₈N₃O₅S, 446.1755 [M-H⁻]; found, 446.1743.

4.2.44. (3*R*,4*R*,5*S*)-4-acetamido-5-(((3-(5-chloro-2-methylphenyl)isoxazol-5-yl)methyl)amino)-3-(pentan-3-yloxy)cyclohex-1-ene-1-carboxylic acid (**17h**)

Yield 55 %; white solid. ¹H NMR (400 MHz, DMSO) δ 7.76 (d, *J* = 9.1 Hz, 1H), 7.58 (d, *J* = 4.0 Hz, 1H), 7.30 (d, *J* = 4.0 Hz, 1H), 6.83 (s, 1H), 6.56 (s, 1H), 3.98 (d, *J* = 7.9 Hz, 1H), 3.79 (dd, *J* = 28.5, 14.7 Hz, 2H), 3.65 (dd, *J* = 18.6, 9.2 Hz, 1H), 3.37 – 3.29 (m, 1H), 2.72 – 2.62 (m, 2H), 2.04 – 1.93 (m, 1H), 1.85 (s, 3H), 1.51 – 1.31 (m, 4H), 0.83 (t, *J* = 7.4 Hz, 3H), 0.79 (t, *J* = 7.4 Hz, 3H). ¹³C NMR (101 MHz, DMSO) δ 170.1, 165.0, 163.0, 137.1, 131.6, 129.0, 127.9, 127.9, 100.4, 81.2, 75.9, 54.8, 41.4, 31.1, 26.1, 25.6, 23.5, 9.9, 9.4. HRMS (ESI, *m/z*) calcd for C₂₂H₂₇ClN₃O₅S, 480.1365 [M-H⁻]; found, 480.1355.

Acknowledgments

The research was supported by Hong Kong RGC Early Career Scheme grant No. 25100017 (C.M.), the State Key Laboratory of Chemical Biology and Drug Discovery, HKPU (C.M.), Hong Kong RGC General Research Fund GRF No. 14165917 (X.Y.), Hong Kong Food and Health Bureau HMRF Grant No. 17160152 (X.Y.) and CU Faculty of Medicine Faculty Innovation Award No. FIA2018/A/03 (X.Y.).

Notes

The authors declare no competing financial interest.

References

- [1] F.G. Hayden, P. Palese, Influenza virus, in: *Clinical Virology*, third Ed., American Society of Microbiology, 2009, pp. 943–976.
- [2] R.G. Webster, W.J. Bean, O.T. Gorman, T.M. Chambers, Y. Kawaoka, Evolution and ecology of influenza A viruses, *Microbiol. Rev.* 56 (1992) 152-179.
- [3] N. Lee, P.K.S. Chan, D.S.C. Hui, T.H. Rainer, E. Wong, K.-W. Choi, G.C.Y. Lui, B.C.K. Wong, R.Y.K. Wong, W.-Y. Lam, I.M.T. Chu, R.W.M. Lai, C.S. Cockram, J.J.Y. Sung, Viral loads and duration of viral shedding in adult patients hospitalized with influenza, *J. Infect. Dis.* 200 (2009) 492–500.
- [4] Centers for Disease Control and Prevention, Seasonal flu death estimate increases worldwide. <https://www.cdc.gov/media/releases/2017/p1213-flu-death-estimate.html>, 2017 (accessed 29 Apr 2019).
- [5] W.C. Cockburn, P.J. Delon, W. Ferreira, Origin and progress of the 1968-69 Hong

- Kong influenza epidemic, *Bull. World Health Organ.* 41 (1969) 345–348.
- [6] J.W. Tang, K.L.K. Ngai, J.C.L. Wong, W.Y. Lam, P.K.S. Chan, Emergence of adamantane-resistant influenza A (H3N2) viruses in Hong Kong between 1997 and 2006, *J. Med. Virol.* 80 (2008) 895–901.
- [7] M.J. Memoli, B.W. Jagger, V.G. Dugan, L. Qi, J.P. Jackson, J.K. Taubenberger, Recent Human Influenza A/H3N2 Virus Evolution Driven by Novel Selection Factors in Addition to Antigenic Drift, *J. Infect. Dis.* 200 (2009) 1232–1241.
- [8] H. Yu, R.-H. Hua, Q. Zhang, T.-Q. Liu, H.-L. Liu, G.-X. Li, G.-Z. Tong, Genetic Evolution of Swine Influenza A (H3N2) Viruses in China from 1970 to 2006, *J. Clin. Microbiol.* 46 (2008) 1067–1075.
- [9] K. McClellan, C.M. Perry, Oseltamivir: A review of its use in influenza, *Drugs.* 61 (2001) 263–283.
- [10] B. Freund, S. Gravenstein, M. Elliott, I. Miller, Zanamivir. A review of clinical safety, *Drug Saf.* 21 (1999) 267–281.
- [11] S. Kubo, T. Tomozawa, M. Kakuta, A. Tokumitsu, M. Yamashita, Laninamivir prodrug CS-8958, a long-acting neuraminidase inhibitor, shows superior anti-influenza virus activity after a single administration, *Antimicrob. Agents Chemother.* 54 (2010) 1256–1264.
- [12] N. Anuwongcharoen, W. Shoombuatong, T. Tantimongcolwat, V. Prachayasittikul, C. Nantasenamat, Exploring the chemical space of influenza neuraminidase inhibitors, *PeerJ.* 4 (2016), e1958.
- [13] A. Moscona, Global transmission of oseltamivir-resistant influenza, *N. Engl. J.*

Med. 360 (2009) 953–956.

[14] R.J. Russell, L.F. Haire, D.J. Stevens, P.J. Collins, Y.P. Lin, G.M. Blackburn, A.J. Hay, S.J. Gamblin, J.J. Skehel, The structure of H5N1 avian influenza neuraminidase suggests new opportunities for drug design, *Nature*. 443 (2006) 45–49.

[15] Y. Wu, G. Qin, F. Gao, Y. Liu, C.J. Vavricka, J. Qi, H. Jiang, K. Yu, G.F. Gao, Induced opening of influenza virus neuraminidase N2 150-loop suggests an important role in inhibitor binding. *Sci. Rep.* 3 (2013) 1551.

[16] Y. Xie, D. Xu, B. Huang, X. Ma, W. Qi, F. Shi, X. Liu, Y. Zhang, W. Xu, Discovery of N-substituted oseltamivir derivatives as potent and selective inhibitors of H5N1 influenza neuraminidase, *J. Med. Chem.* 57 (2014) 8445–8458.

[17] J. Zhang, V. Poongavanam, D. Kang, C. Bertagnin, H. Lu, X. Kong, H. Ju, X. Lu, P. Gao, Y. Tian, H. Jia, S. Desta, X. Ding, L. Sun, Z. Fang, B. Huang, X. Liang, R. Jia, X. Ma, W. Xu, N.A. Murugan, A. Loregian, B. Huang, P. Zhan, X. Liu, Optimization of N-substituted oseltamivir derivatives as potent inhibitors of group-1 and -2 influenza A neuraminidases, including a drug-resistant variant, *J. Med. Chem.* 61 (2018) 6379–6397.

[18] J. Zhang, N.A. Murugan, Y. Tian, C. Bertagnin, Z. Fang, D. Kang, X. Kong, H. Jia, Z. Sun, R. Jia, P. Gao, V. Poongavanam, A. Loregian, W. Xu, X. Ma, X. Ding, B. Huang, P. Zhan, X. Liu, Structure-based optimization of N-substituted oseltamivir derivatives as potent anti-influenza A virus agents with significantly improved potency against oseltamivir-resistant N1-H274Y variant, *J. Med. Chem.* 61 (2018) 9976–9999.

[19] P.J.P. Adabala, E.B. Legresley, N. Bance, M. Niikura, B.M. Pinto, Exploitation of

the catalytic site and 150 cavity for design of influenza A neuraminidase inhibitors, *J. Org. Chem.* 78 (2013) 10867–10877.

[20] S. Mohan, S. McAtamney, T. Haselhorst, M. Von Itzstein, B.M. Pinto, Carbocycles related to oseltamivir as influenza virus group-1-specific neuraminidase inhibitors. Binding to N1 enzymes in the context of virus-like particles, *J. Med. Chem.* 53 (2010) 7377–7391.

[21] R.X. Gu, L.A. Liu, D.Q. Wei, Structural and energetic analysis of drug inhibition of the influenza A M2 proton channel, *Trends Pharmacol. Sci.* 34 (2013) 571–580.

[22] J. Wang, C. Ma, J. Wang, H. Jo, B. Canturk, G. Fiorin, L.H. Pinto, R.A. Lamb, M.L. Klein, W.F. DeGrado, Discovery of novel dual inhibitors of the wild-type and the most prevalent drug-resistant mutant, S31N, of the M2 proton channel from influenza A virus, *J. Med. Chem.* 56 (2013) 2804–2812.

[23] F. Li, C. Ma, W.F. Degrado, J. Wang, Discovery of highly potent inhibitors targeting the predominant drug-resistant S31N mutant of the influenza A virus M2 proton channel, *J. Med. Chem.* 59 (2016) 1207–1216.

[24] Y. Wang, Y. Hu, S. Xu, Y. Zhang, R. Musharrafieh, R.K. Hau, C. Ma, J. Wang, In vitro pharmacokinetic optimizations of AM2-S31N channel blockers led to the discovery of slow-binding inhibitors with potent antiviral activity against drug-resistant influenza A viruses, *J. Med. Chem.* 61 (2018) 1074–1085.

[25] M. Okomo-Adhiambo, T.G. Sheu, L.V. Gubareva, Assays for monitoring susceptibility of influenza viruses to neuraminidase inhibitors, *Influenza Other Respir. Viruses.* 7 (2013) 44–49.

[26] M. Tonelli, S. Espinoza, R.R. Gainetdinov, E. Cichero, Novel biguanide-based derivatives scouted as TAAR1 agonists: Synthesis, biological evaluation, ADME prediction and molecular docking studies, *Eur. J. Med. Chem.* 127 (2017) 781–792.

[27] C. Tintori, M. Magnani, S. Schenone, M. Botta, Docking, 3D-QSAR studies and in silico ADME prediction on c-Src tyrosine kinase inhibitors, *Eur. J. Med. Chem.* 44 (2009) 990–1000.